Molecular Dynamics Study of Phase Separation Kinetics in Thin Films

Subir K. Das,[1] Sanjay Puri,[2] Jürgen Horbach,[1] and K. Binder[1]
[1]*Institut für Physik, Johannes Gutenberg-Universität, D-55099 Mainz, Staudinger Weg 7, Germany*
[2]*School of Physical Sciences, Jawaharlal Nehru University, New Delhi 110067, India*
(Received 4 October 2005; published 12 January 2006)

We use molecular dynamics to simulate experiments where a symmetric binary fluid mixture (AB), confined between walls that preferentially attract one component (A), is quenched from the one-phase region into the miscibility gap. Surface enrichment occurs during the early stages, yielding a B-rich mixture in the film center with well-defined A-rich droplets. The droplet size grows with time as $\ell(t) \propto t^{2/3}$ after a transient regime. The present atomistic model is also compared to mesoscopic coarse-grained models for this problem.

DOI: 10.1103/PhysRevLett.96.016107 PACS numbers: 68.05.−n, 64.75.+g, 68.08.Bc, 68.15.+e

Understanding the dynamics of phase changes, such as the kinetics of unmixing of binary systems (*spinodal decomposition* [1]), has been a long-standing challenge [1–17]. In particular, the effect of hydrodynamic interactions on the intermediate and late stages of coarsening in phase-separating fluid mixtures is an intriguing problem. For off-critical compositions, well-separated droplets occur with a size $\ell(t)$ that is predicted to grow as $\ell(t) \propto t^{1/3}$ in $d = 3$—according to both the evaporation-condensation mechanism [2] and the droplet diffusion and coagulation mechanism [3]. However, in $d = 2$, droplet coagulation yields $\ell(t) \propto t^{1/2}$ [3], while the Lifshitz-Slyozov mechanism [2] still gives $\ell(t) \propto t^{1/3}$. For compositions where the domain structures are bicontinuous, hydrodynamic mechanisms yield $\ell(t) \propto t$ in $d = 3$ [6,8], and $\ell(t) \propto t^{1/2}$ in $d = 2$ [7] for $\ell(t) \ll$ inertial length $L_{\rm in} \simeq \eta^2/(\rho\gamma)$. Here, η is the shear viscosity, ρ is the fluid density, and γ is the interfacial tension between A-rich and B-rich domains. For $\ell(t) \gg L_{\rm in}$, the law $\ell(t) \propto (\gamma/\rho)^{1/3} t^{2/3}$ is expected in both $d = 2, 3$ [8]. But experiments and simulations often find slow transients before these asymptotic power laws occur, and this transient behavior is less well understood [14–17]. In particular, for $d = 2$, it is still controversial whether a scaling description in terms of universal power laws holds at all [13]. Also arguments that the growth exponent should not exceed $1/2$ due to turbulent remixing are discussed in the literature [18,19].

Recently, much attention has focused on phase separation near surfaces with a preferential attraction for one of the components of the mixture [20–25]. In this problem, an interesting interplay occurs between lateral phase separation (parallel to the surface) and the formation of a stratified structure in the perpendicular direction. This phenomenon is usually referred to as surface-directed spinodal decomposition (SDSD) and has important technological applications. However, the interplay between wetting and unmixing causes intricate transients and crossovers in the growth laws, which are not well understood. Experiments often do not provide information on both lateral and perpendicular concentration variations. Moreover, most simulations have used models without hydrodynamic interactions [21–23,25], though there are a few studies of SDSD in fluid mixtures [26–29].

Here we present atomistic simulations of SDSD in thin films, using molecular dynamics (MD) for a symmetric Lennard-Jones (LJ) mixture [30]—thereby hydrodynamic effects are automatically included. Since MD is restricted to length scales ~10 nm and time scales ~10 ns [31], we compare our results to data for the initial stages of SDSD in a coarse-grained model [23].

Following Das *et al.* [32], the binary fluid has point particles interacting with LJ potentials:

$$u(r_{ij}) = 4\epsilon_{\alpha\beta}\left[\left(\frac{\sigma}{r_{ij}}\right)^{12} - \left(\frac{\sigma}{r_{ij}}\right)^{6}\right], \qquad (1)$$

where $r_{ij} = |\vec{r}_i - \vec{r}_j|$; $\alpha, \beta = A, B$. We set $\epsilon_{AA} = \epsilon_{BB} = \epsilon$, $\epsilon_{AB} = \epsilon/2$. These potentials are truncated at $r_{ij} = 2.5\sigma$ and then shifted to zero. We consider the case of a critical quench, with equal numbers of A and B particles. Their masses are equal, $m_A = m_B = m = 1$, and units are chosen such that $\sigma = 1$, $\epsilon = 1$, $k_B = 1$. Working at a density $\rho = 1$, phase separation sets in at a critical temperature $T_c = 1.638$ [32] in the bulk fluid, well separated from the gas-liquid and liquid-solid transitions.

The particles were confined in a rectangular box of size $L \times L \times D$, with $D = 5$, $L = 128$ ($N = 98\,304$ particles); $D = 10$, $L = 64$ ($N = 45\,056$); $D = 20$, $L = 64$ ($N = 86\,016$). Periodic boundary conditions were applied in the x and y directions, which are parallel to the walls located at $z = 0$ and $z = D$. The walls give rise to an integrated LJ potential u_w:

$$u_w = \frac{2\pi\rho\sigma^3}{3}\epsilon_w\left[\frac{2}{15}\left(\frac{\sigma}{z'}\right)^9 - \delta_\alpha\left(\frac{\sigma}{z'}\right)^3\right]. \qquad (2)$$

We choose $\delta_A = 1$, $\delta_B = 0$, so there is only a repulsion for the B particles. Further, $z' = z + \sigma/2$ for the wall at $z = 0$, and $z' = D + \sigma/2 - z$ for the wall at $z = D$. This corresponds to a symmetric film with identical walls. Finally, $\epsilon_w = 0.005$, which corresponds to a partially wet (PW) state at the temperature $T = 1.1$ considered in our

quenches. At this temperature, the bulk correlation length is $\xi \simeq 1$ [32], facilitating a comparison with the Ginzburg-Landau (GL) model described below, where lengths are measured in units of ξ [21–23,25]. Further, at this temperature, segregation between A and B is complete [32]. Finally, the viscosity and surface tension are $\eta \simeq 7$ and $\gamma \simeq 0.9$ [32].

The MD runs were performed using the standard velocity Verlet algorithm [34], with a time step $\Delta t = 0.02$ in MD units $\tau = (m\sigma^2/48\epsilon)^{1/2}$, and the Nosé-Hoover thermostat [34]. Initial configurations are equilibrated at $T = 5$ (where the A and B particles are randomly mixed) for 10^5 time steps. We averaged data over three independent quenches to improve the statistics.

The GL model considered here describes diffusion-driven segregation in thin films [23]. It consists of the dimensionless Cahn-Hilliard-Cook equation for the order parameter $\psi \propto n_A - n_B$,

$$\frac{\partial}{\partial t}\psi(\vec{r}, t) = \nabla^2\left[-\psi + \psi^3 - \frac{1}{2}\nabla^2\psi + V(z)\right] + \vec{\nabla}\cdot\vec{\theta}, \tag{3}$$

where $0 < z < D$. We set $\vec{r} = (\vec{\rho}, z)$, where $\vec{\rho}$ denotes the coordinates parallel to the surface. We consider symmetric power-law potentials, $V(z) = -V_0[(z+1)^{-3} + (D+1-z)^{-3}]$, which corresponds to a nonretarded van der Waals' interaction in $d = 3$ between the surfaces at $z = 0, D$ and a particle. The order parameter is driven by a conserved Gaussian white noise $\vec{\nabla}\cdot\vec{\theta}$. Equation (3) must be supplemented by two boundary conditions wherever a surface is introduced. The first boundary condition at $z = 0$ accounts for the relaxation of the order parameter at the surface:

$$0 = h_1 + g\psi(\vec{\rho}, 0, t) + \gamma\frac{\partial\psi}{\partial z}\bigg|_{z=0}, \tag{4}$$

where $h_1 = -V(0)$, and g, γ are parameters [23,25]. The second boundary condition at $z = 0$ is the no-flux condition:

$$0 = \left\{\frac{\partial}{\partial z}\left[-\psi + \psi^3 - \frac{1}{2}\nabla^2\psi + V(z)\right] + \theta_z\right\}_{z=0}. \tag{5}$$

Similar boundary conditions are applied at $z = D$. We implemented a Euler-discretized version of the GL model on an $L \times L \times D$ lattice. The discretization mesh sizes were $\Delta x = 1$ and $\Delta t = 0.02$. The parameter values were $g = -0.4$, $\gamma = 0.4$, and $V_0 = 0.11$, corresponding to a PW equilibrium morphology [23].

In Figs. 1(a) and 1(c), we show the evolution of the average depth profile $\psi_{\rm av}(z, t)$ vs z, obtained from the MD simulations for $D = 5, 10$. This quantity is defined in terms of the local densities (n_A, n_B) as $\psi_{\rm av} = (n_A - n_B)/(n_A + n_B)$, and is averaged in the directions parallel to the surface. The corresponding depth profiles for the GL model are shown in Figs. 1(b) and 1(d). The local concentration at the surfaces equilibrates rapidly for both the MD and GL models. Because of the enhancement of $\psi_{\rm av}(z, t)$ near the surfaces, an adjacent depletion layer forms, which propagates into the bulk. In the later stages, these SDSD waves coalesce, so the profiles have a single minimum in the center of the film. This is already seen to have happened for the $D = 5$ profiles in Figs. 1(a) and 1(b).

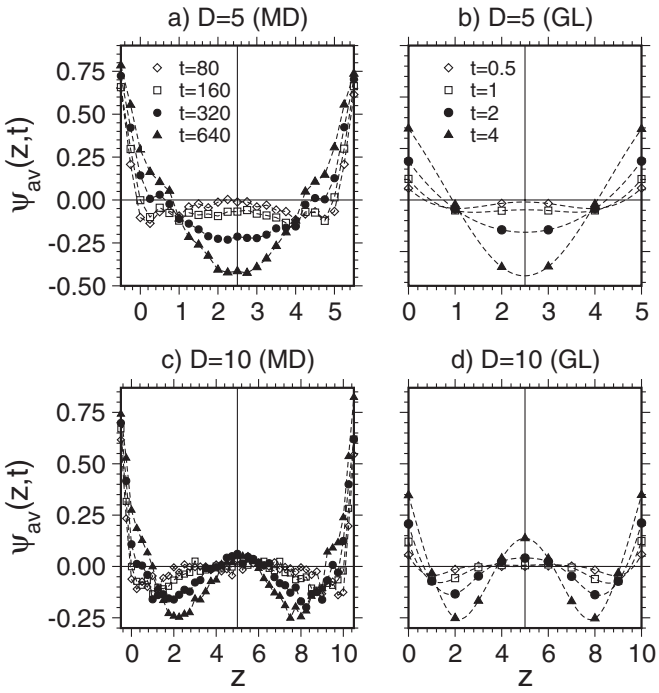

FIG. 1. Laterally averaged depth profiles, $\psi_{\rm av}(z, t)$ vs z, obtained from the MD and GL simulations described in the text. We show profiles at different times for (a) $D = 5$ (MD), (b) $D = 5$ (GL), (c) $D = 10$ (MD), and (d) $D = 10$ (GL). The GL data were obtained as an average over 5 independent runs with $L = 256$.

In the GL case [23], a metastable layered state is established by the coalescence of SDSD waves arising from both surfaces—regardless of whether the equilibrium morphology is PW or completely wet (CW). This metastable state breaks up into a columnar coarsening structure but can be rather long-lived, depending on the proximity to the PW $\rightarrow$ CW boundary and the film thickness. We see no evidence of a transient layered state in our MD simulations, indicating that hydrodynamic mechanisms accelerate the onset of the asymptotic regime.

The comparison between the MD and GL models can only be qualitative, even during the early stages of the quench where the hydrodynamic effects in the MD case are not yet operative. There are several reasons for this: (a) the strength and range of the wall potentials differ in both models; (b) it is not straightforward to map the MD time unit to that of the GL model; and (c) the coarse spatial discretization of the latter does not permit resolution of fine structural details that are visible in the former. Nevertheless, Fig. 1 suggests that a quantitative comparison should be feasible with some refinements, e.g., finer spatial resolution, optimization of the choice of the wall potential in the GL model, etc. Notice that a comparison on longer

time scales necessitates the incorporation of a hydrodynamic flow field in the GL model, i.e., a study of *Model H* [35] in a confined geometry [26]. An alternative approach is to compare our MD results with those from a (mesoscopic) lattice Boltzmann (LB) model, where hydrodynamic effects are already included [13,14]. From the comparison in Fig. 1, it is clear that MD work is much more demanding than GL, since about 160 MD time units (τ) are needed to reach about the same structures of the films as in the GL work for $t = 1$. This large number of MD time units is roughly understood from the structural relaxation time, which can be estimated from the viscosity [32] as ≈ 7 LJ units $\approx 50\tau$.

To understand the intermediate and late stages of coarsening, the evolution of the concentration in the central plane of the film is illuminating. In Fig. 2, we show the corresponding snapshots from our MD simulation for $D = 10$. For $t \leq 10^3$, the morphology is approximately bicontinuous. However, at later times, the growth of the enrichment layers at the walls depletes the central region of the films so much that the A-rich regions break up into well-separated droplets. These droplets extend in the z direction throughout the film, and are thus connected with each other through the enrichment layers.

Next, we examine the layerwise correlation function $C(\rho, z, t)$ in the direction parallel to the surfaces. Figure 3 is a scaling plot of $C(\rho, z, t)/C(0, z, t)$ vs $\rho/\ell(z, t)$ for $z = D/2$. Here, the characteristic length $\ell(z, t)$ is defined as $C(\ell, z, t) = C(0, z, t)/2$. For the $D = 5$ case [Fig. 3(a)], the early-time data ($t = 80, 800$) correspond to a time regime where the average composition in the central region is changing [see Fig. 1(a)]—hence, the data do not satisfy scaling. The data for later times ($t = 4000, 8000$) correspond to a regime where columnar structures are well established, and these undergo lateral coarsening. In this regime, dynamical scaling is restored. Similar arguments apply for the $D = 10$ case [Fig. 3(b)], but it takes longer to reach the columnar coarsening regime. Thus, the data sets in Fig. 3(b) show a crossover behavior.

Finally, in Fig. 4, we show the time dependence of the lateral length scales for values of z ranging from the surface ($z = 0$) to the film center. In the asymptotic regime, all data sets are consistent with the inertial growth law $\ell(t) \propto t^{2/3}$. Note, however, that only one decade of time is at our disposal. Given the caveats about scaling in 2D spinodal decomposition of fluids [13], it is not clear that the true asymptotic regime has been reached. Though there are fundamental differences between our quasi-2D system and strictly 2D systems, the qualitative similarity of our results (Fig. 4) to the Brownian dynamics simulations of Farrell and Valls [11] is striking.

In conclusion, we have demonstrated the feasibility of atomistic MD simulations of SDSD in thin films. These are complementary to mesoscopic approaches, which involve the simulation of coarse-grained GL models or LB models. A key feature of our results is the interplay between lateral phase separation and the formation of enrichment layers at

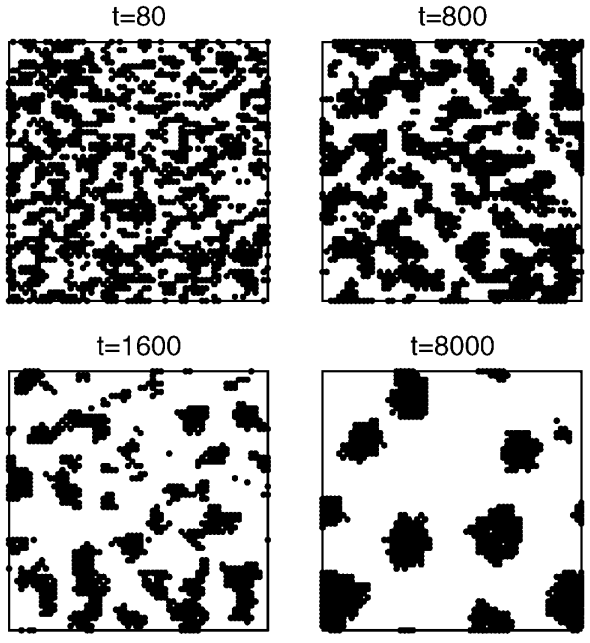

FIG. 2. Evolution snapshots (obtained from MD) of the concentration in the center layer of the thin film with $D = 10$. A coarse graining was done, dividing the systems into cells of size $(2\sigma)^2$. Cells with a majority of A particles are marked in black, and other cells are unmarked.

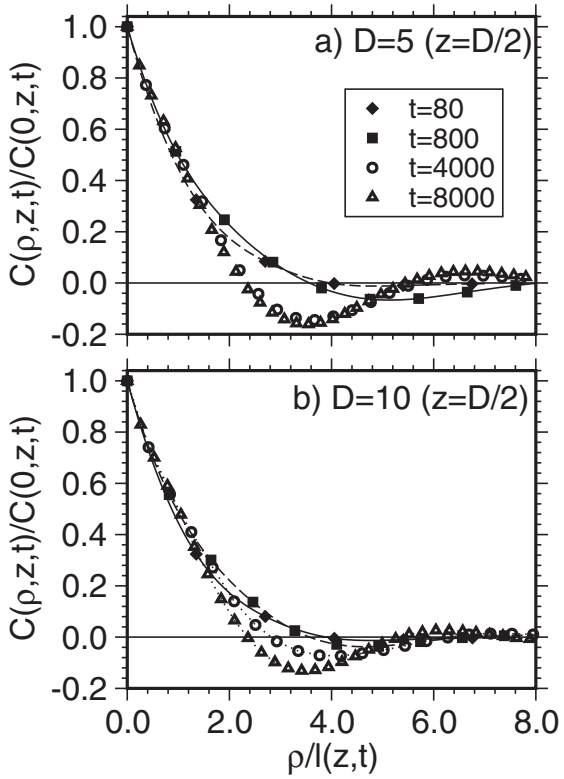

FIG. 3. Scaling plot of layerwise correlation functions, at the center of the film. We plot $C(\rho, z, t)/C(0, z, t)$ vs $\rho/\ell(z, t)$ at different times for (a) $D = 5$, (b) $D = 10$.

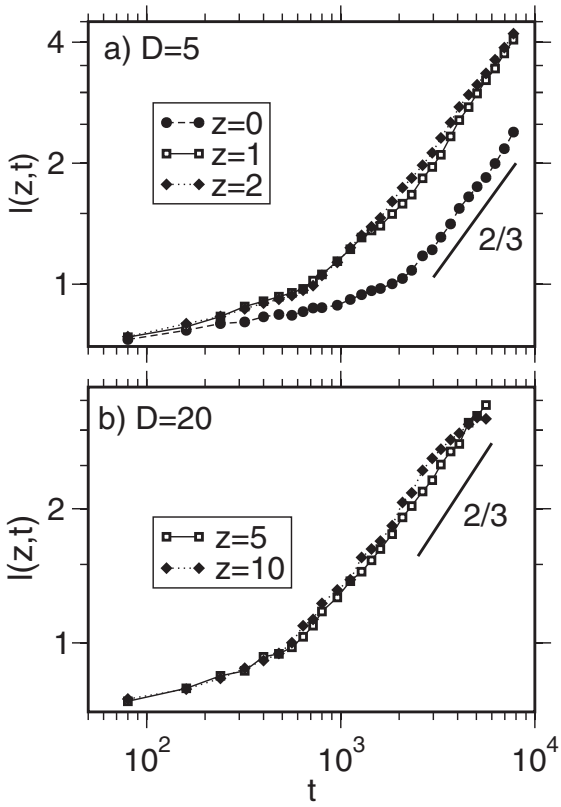

FIG. 4. Time dependence of layerwise length scale, $\ell(z, t)$ vs t, plotted on a log-log scale. We show data for different values of z, and (a) $D = 5$, (b) $D = 20$.

the walls. This gives rise to a complex crossover behavior, which we have clarified through MD and GL simulations. We hope that our results will help to understand experiments on this problem, and stimulate analytical work on this subject.

We thank the Deutsche Forschungsgemeinschaft (DFG) for support via Grant No. Bi 314/18-2 (S. K. D.), the Emmy Noether Program (J. H.), and Grant No. SFB 625/A3 (S. P.).

[1] J. W. Cahn, Acta Metall. **9**, 795 (1961).
[2] I. M. Lifshitz and V. V. Slyozov, J. Phys. Chem. Solids **19**, 35 (1961).
[3] K. Binder and D. Stauffer, Phys. Rev. Lett. **33**, 1006 (1974).
[4] J. S. Langer, M. Bar-on, and H. D. Miller, Phys. Rev. A **11**, 1417 (1975).
[5] K. Kawasaki and T. Ohta, Prog. Theor. Phys. **59**, 362 (1978).
[6] E. D. Siggia, Phys. Rev. A **20**, 595 (1979).
[7] M. San Miguel, M. Grant, and J. D. Gunton, Phys. Rev. A **31**, 1001 (1985).
[8] H. Furukawa, Phys. Rev. A **31**, 1103 (1985); **36**, 2288 (1987).
[9] Y. Oono and S. Puri, Phys. Rev. Lett. **58**, 836 (1987); Phys. Rev. A **38**, 434 (1988); S. Puri and Y. Oono, Phys. Rev. A **38**, 1542 (1988).
[10] S. Puri and B. Dünweg, Phys. Rev. A **45**, R6977 (1992).
[11] J. E. Farrell and O. T. Valls, Phys. Rev. B **40**, 7027 (1989); **42**, 2353 (1990); **43**, 630 (1991).
[12] T. Koga and K. Kawasaki, Physica (Amsterdam) **196A**, 389 (1993).
[13] F. J. Alexander, S. Chen, and D. W. Grunau, Phys. Rev. B **48**, 634 (1993); A. J. Wagner and J. M. Yeomans, Phys. Rev. Lett. **80**, 1429 (1998); H. Furukawa, Phys. Rev. E **61**, 1423 (2000); A. J. Wagner and M. E. Cates, Europhys. Lett. **56**, 556 (2001).
[14] V. M. Kendon, J.-C. Desplat, P. Bladon, and M. E. Cates, Phys. Rev. Lett. **83**, 576 (1999); V. M. Kendon, M. E. Cates, I. Pagonabarraga, J.-C. Desplat, and P. Bladon, J. Fluid Mech. **440**, 147 (2001).
[15] A. J. Bray, Adv. Phys. **43**, 357 (1994).
[16] K. Binder and P. Fratzl, in *Phase Transformations in Materials*, edited by G. Kostorz (Wiley-VCH, Weinheim, New York, 2001), p. 409.
[17] A. Onuki, *Phase Transition Dynamics* (Cambridge University Press, Cambridge, 2002).
[18] M. Grant and K. R. Elder, Phys. Rev. Lett. **82**, 14 (1999).
[19] P. B. Warren, Phys. Rev. Lett. **87**, 225702 (2001).
[20] R. A. L. Jones, L. J. Norton, E. J. Kramer, F. S. Bates, and P. Wiltzius, Phys. Rev. Lett. **66**, 1326 (1991).
[21] S. Puri and K. Binder, Phys. Rev. A **46**, R4487 (1992); Phys. Rev. E **49**, 5359 (1994).
[22] S. Puri and K. Binder, Phys. Rev. Lett. **86**, 1797 (2001); Phys. Rev. E **66**, 061602 (2002).
[23] S. K. Das, S. Puri, J. Horbach, and K. Binder, Phys. Rev. E **72**, 061603 (2005).
[24] For reviews of experiments, see G. Krausch, Mater. Sci. Eng., R **14**, v (1995); M. Geoghegan and G. Krausch, Prog. Polym. Sci. **28**, 261 (2003).
[25] For reviews of the phenomenological modeling, see S. Puri and H. L. Frisch, J. Phys. Condens. Matter **9**, 2109 (1997); K. Binder, J. Non-Equilib. Thermodyn. **23**, 1 (1998); S. Puri, J. Phys. Condens. Matter **17**, R1 (2005).
[26] H. Tanaka, J. Phys. Condens. Matter **13**, 4637 (2001).
[27] S. Bastea, S. Puri, and J. L. Lebowitz, Phys. Rev. E **63**, 041513 (2001).
[28] W.-J. Ma, P. Keblinski, A. Maritan, J. Koplik, and J. R. Banavar, Phys. Rev. E **48**, R2362 (1993).
[29] S. Toxvaerd, Phys. Rev. Lett. **83**, 5318 (1999).
[30] For the 2D case, a similar model was studied by E. Velasco and S. Toxvaerd, Phys. Rev. Lett. **71**, 388 (1993), but it was not possible to conclusively determine the growth behavior. See also P. Ossadnik *et al.*, Phys. Rev. Lett. **72**, 2498 (1994), who suggest $\ell(t) \propto t^{1/2}$.
[31] *Bridging Time Scales: Molecular Simulations for the Next Decade*, edited by P. Nielaba, M. Mareschal, and G. Cicotti (Springer, Berlin, 2002).
[32] S. K. Das, J. Horbach, and K. Binder, J. Chem. Phys. **119**, 1547 (2003).
[33] K. Binder, J. Baschnagel, W. Kob, and W. Paul, in [31], p. 169.
[34] *Monte Carlo and Molecular Dynamics of Condensed Matter Systems*, edited by K. Binder and G. Ciccotti (Italian Physical Society, Bologna, 1996).
[35] P. C. Hohenberg and B. I. Halperin, Rev. Mod. Phys. **49**, 435 (1977).